

Universal width distributions in non-Markovian Gaussian processes

This article has been downloaded from IOPscience. Please scroll down to see the full text article.

J. Stat. Mech. (2007) P02009

(<http://iopscience.iop.org/1742-5468/2007/02/P02009>)

View [the table of contents for this issue](#), or go to the [journal homepage](#) for more

Download details:

IP Address: 129.175.97.14

The article was downloaded on 22/09/2010 at 15:13

Please note that [terms and conditions apply](#).

Universal width distributions in non-Markovian Gaussian processes

Raoul Santachiara^{1,2}, Alberto Rosso³ and Werner Krauth⁴

¹ CNRS-Laboratoire de Physique Théorique, Université Louis Pasteur, 3 rue de l'Université, F-67084 Strasbourg Cedex, France

² CNRS-Laboratoire de Physique Théorique, Ecole Normale Supérieure, 24 rue Lhomond, F-75231 Paris Cedex 05, France

³ CNRS-Laboratoire de Physique Théorique et Modèles Statistiques, Bâtiment 100 Université Paris-Sud, F-91405 Orsay Cedex, France

⁴ CNRS-Laboratoire de Physique Statistique, Ecole Normale Supérieure, 24 rue Lhomond, F-75231 Paris Cedex 05, France

E-mail: raoul.santachiara@lpt.ens.fr, rosso@lptms.u-psud.fr and krauth@lps.ens.fr

Received 21 November 2006

Accepted 18 January 2007

Published 8 February 2007

Online at stacks.iop.org/JSTAT/2007/P02009

doi:[10.1088/1742-5468/2007/02/P02009](https://doi.org/10.1088/1742-5468/2007/02/P02009)

Abstract. We study the influence of boundary conditions on self-affine random functions $u(t)$ in the interval $t \in [0, L]$, with independent Gaussian Fourier modes q of variance $\sim 1/q^\alpha$. We consider the probability distribution of the mean square width of $u(t)$ taken over the whole interval or in a window $t/L \in [x, x + \delta]$. Its characteristic function can be expressed in terms of the spectrum of an infinite matrix. This distribution strongly depends on the boundary conditions of $u(t)$ for finite δ , but we show that it is universal (independent of boundary conditions) in the small-window limit ($\delta \rightarrow 0$, $\delta \ll \min[x, 1 - x]$). We compute it directly for arbitrary $\alpha > 1$, using, for $\alpha < 3$, an asymptotic expansion formula that we derive. For $\alpha > 3$, the limiting width distribution is independent of α . It corresponds to an infinite matrix with a single non-zero eigenvalue. We give the exact expression for the width distribution in this case. Our calculation allows us to extract the roughness exponent from the width distribution of experimental data even in cases where the standard extrapolation method cannot be used.

Keywords: self-affine roughness (theory), Brownian motion, stochastic processes (theory)

ArXiv ePrint: [cond-mat/0611326](https://arxiv.org/abs/cond-mat/0611326)

Contents

1. Introduction	2
2. Average width	6
2.1. Average width for $\delta = 1$	6
2.2. Average width for $\delta < 1$	7
2.3. Small-window limit	9
3. Width distribution	10
3.1. Width distribution for the entire interval ($\delta = 1$)	11
3.2. Width distribution for windows (finite δ)	12
3.3. Width distribution in the small-window limit	13
3.3.1. Small-window limit ($\alpha < 3$).	13
3.3.2. Small-window limit ($\alpha \geq 3$).	15
4. Conclusions	16
Acknowledgments	17
Appendix A. Expansion formula	17
A.1. Expansion formula for non-integer α	17
A.2. Expansion formula for integer α	19
Appendix B. General cumulants	20
References	21

1. Introduction

In nature, random processes model interfaces and surfaces [1, 2], turbulent flows [3], erratic time series [4] and many other systems. In the most simple setting, these random processes correspond to a function of a scalar variable $u(t)$, and are characterized by a probability distribution $\mathcal{P}[u(t)]$ that stems from an equilibrium problem or a non-equilibrium process. The probability distribution $\mathcal{P}[u(t)]$ is often unknown, and generally inaccessible to exact analysis. In many cases, approximate methods must be brought to bear on these problems.

One of the most successful approaches in the field of random processes is the Gaussian approximation. It consists in writing the function $u(t)$ in the interval $t \in [0, L]$ in Fourier space schematically as

$$u(t) \sim \sum_{n=-\infty}^{\infty} a_n \exp(iq_n t), \tag{1}$$

with modes $q_n \propto n/L$ and in assuming that the coefficients $a_n = a_{-n}^*$ are independent Gaussian random variables (see equations (2)–(4) for precise definitions). The probability distribution $\mathcal{P}[u(t)] = \mathcal{P}[\{a_1, a_2, \dots\}]$ then factorizes into a product $\mathcal{P} \simeq \mathcal{P}^{\text{Gauss}} = \mathcal{P}^{\text{Gauss}}(a_1)\mathcal{P}^{\text{Gauss}}(a_2)\dots$, where $\mathcal{P}^{\text{Gauss}}(a_n)$ is a Gaussian with zero mean and variance σ_n^2 . The idea behind the Gaussian approximation is to replace the translation-invariant

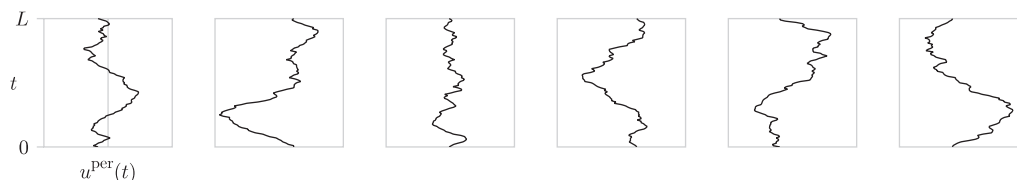


Figure 1. Gaussian functions $u^{\text{per}}(t)$ in the interval $t \in [0, L]$, corresponding to a probability distribution $\mathcal{P}^{\text{Gauss}}[u^{\text{per}}(t)]$ with $\zeta = 0.75$ ($\alpha = 2.5$) (full periodic series).

action of a complicated interacting problem by a quadratic (Gaussian) action which yields the same two-point correlation functions as in the original problem. In the particularly important case of self-affine (critical) systems, the only length scale present is the system size. The scaling of the variances σ_n^2 with the modes q_n can then be described by a single parameter α with $\sigma_n^2 \propto 1/n^\alpha$ ($\alpha > 1$). In many non-trivial problems, the Gaussian approximation is in outstanding quantitative agreement with the full theory [5, 6] and reproduces very well even the higher-order correlation functions.

Because of its decoupled Fourier modes, the Gaussian approximation is considerably simpler than the full theory and the function $u(t)$ can easily be generated through equation (1) from Gaussian random numbers $\{a_n\}$ (see figure 1). However, the price to pay for this simplicity in Fourier space is to have non-trivial long-range correlations in real space. As we will discuss in detail, the real-space action contains generalized derivatives which, in the sense of the Riemann–Liouville derivative, can be expressed as an integral convolution with a long-range kernel [7]. For non-integer values of $\alpha/2$, the real-space Gaussian action is non-local and the geometrical properties of the function $u(t)$ are intricate.

For $\alpha = 2$, the Gaussian approximation corresponds to the notorious random walk. In this case the real-space action is local. It defines a Markovian evolution (the value of u at $t + dt$ depends only on the one at t). For this reason it is possible to determine in detail its geometric properties (for a recent review see [8]). For $\alpha \neq 2$, instead, the process $u(t)$ is non-Markovian: in the case $\alpha = 4$ (the driven curvature model [1, 9]), the evolution of the derivative du/dt is Markovian, but not the one of $u(t)$ itself. For non-integer $\alpha/2$, the non-Markovian properties reflect the non-local character of the action. This implies that, generally, memory effects influence the shape of $u(t)$ and calculations, even within the Gaussian approximation, are difficult. In particular, the persistence exponents and the distribution of the extreme remain unknown [10, 11]. On the other hand, the boundary conditions influence the statistical properties of $u(t)$ in a non-trivial way for all $t \in [0, L]$. Understanding these effects is important because the periodic boundary conditions for $u(t)$, which are commonplace in theoretical calculations and in numerical simulations, are usually not realized in experiments [12, 13].

As an example of a fundamental geometrical quantity sensitive to the boundary, we consider the mean square width

$$w_2 = w_2[u(t)] = \frac{1}{L} \int_0^L dt u^2(t) - \frac{1}{L^2} \left[\int_0^L dt u(t) \right]^2,$$

which is relevant both from the theoretical and the experimental points of view. For a self-affine random process, the mean square width is itself described by a non-trivial probability distribution $\mathcal{P}(w_2)$.

In this work, we study the influence of boundary conditions on the width distribution of $\mathcal{P}^{\text{Gauss}}[u(t)]$ for self-affine functions characterized by variances scaling with the single parameter α . In fact, the schematic Fourier representation of equation (1) can be rendered explicit in a number of ways in order to accommodate the boundary conditions. First it can be generated from the full periodic Fourier series,

$$u^{\text{per}}(t) = \sum_{n=1}^{\infty} a_n \cos\left(\frac{2\pi n}{L}t\right) + b_n \sin\left(\frac{2\pi n}{L}t\right) \quad (\text{full periodic series}), \quad (2)$$

where a_n and b_n are independent Gaussian random numbers of variance $[\sigma_n^{\text{per}}]^2 \propto 1/n^\alpha$. This implies that the function $u^{\text{per}}(t)$, which has zero average, and all its derivatives are periodic, if they exist ($[u^{\text{per}}]^{(k)}(t=0) = [u^{\text{per}}]^{(k)}(t=L)$ for $k = 0, 1, \dots \leq \alpha/2$). It is also possible to generate a Gaussian function $u^{\text{sin}}(t)$ from a sine Fourier series,

$$u^{\text{sin}}(t) = \sum_{n=1}^{\infty} s_n \sin\left(\frac{\pi n}{L}t\right) \quad (\text{sine series}), \quad (3)$$

again supposing that the s_n are independent Gaussians with variance $[\sigma_n^{\text{sin}}]^2 \propto 1/n^\alpha$. The function $u^{\text{sin}}(t)$ vanishes at $t = 0$ and $t = L$. By a uniform shift of the function, it can be made to have zero average value, as for the full periodic series. However, all its existing even derivatives vanish ($[u^{\text{sin}}]^{(k)}(0) = [u^{\text{sin}}]^{(k)}(L) = 0$ for $k = 0, 2, \dots \leq \alpha/2$). The full periodic series and the sine series are statistically equivalent for the random walk ($\alpha = 2$) [14, 15], but they differ for all other values of α .

Finally, a function $u^{\text{cos}}(t)$ can also be generated from a cosine Fourier series,

$$u^{\text{cos}}(t) = \sum_{n=1}^{\infty} c_n \cos\left(\frac{\pi n}{L}t\right) \quad (\text{cosine series}), \quad (4)$$

again with $[\sigma_n^{\text{cos}}]^2 \propto 1/n^\alpha$. In this case, the random function is not forced to take the same value at $t = 0$ and at $t = L$, and for this reason it has been used to study free random walks [8]. Analogously to the sine Fourier series, all the odd derivatives of $u^{\text{cos}}(t)$ must vanish at the boundaries, if they exist ($[u^{\text{cos}}]^{(k)}(0) = [u^{\text{cos}}]^{(k)}(L) = 0$ for $k = 1, 3, \dots \leq \alpha/2$). This paper shows that these additional constraints strongly influence the geometry of the function $u^{\text{cos}}(t)$ for $\alpha \neq 2$.

The above three stochastic series correspond to the same real-space action $\mathcal{S}[u(t)]$ and its associated Gaussian probability distribution $\mathcal{P}^{\text{Gauss}}[u(t)]$

$$\mathcal{S}[u(t)] = \frac{1}{2} \int_0^L dt \left(\frac{\partial^{\alpha/2} u(t)}{\partial t^{\alpha/2}} \right)^2 \implies \mathcal{P}^{\text{Gauss}}[u(t)] \propto \exp\{-\mathcal{S}[u(t)]\}. \quad (5)$$

For non-integer values of $\alpha/2$, the generalized derivative in equation (5) is defined in momentum space: $[\partial^{\alpha/2}/\partial t^{\alpha/2}] e^{iqt} = (iq)^{\alpha/2} e^{iqt}$ (the derivative can also be defined in real space [7]).

To arrive from the action equation (5) at the functions $u^{\text{per}}(t)$, $u^{\text{cos}}(t)$, and $u^{\text{sin}}(t)$, we must specify the boundary conditions on the general function $u(t)$ and this makes that the three bases correspond to different stochastic processes. The boundary conditions are actually fixed by requiring the uniform convergence of the (infinite) Fourier series in the interval $[0, L]$: this allows us to exchange in the action equation (5) the $\alpha/2$ derivative with the Fourier sum under consideration and to compute the variances of the Fourier coefficients with the correct normalization. Using the action in equation (5), we obtain:

$$\begin{aligned} [\sigma_n^{\text{per}}]^2 &= \frac{L^{\alpha-1}}{2^{\alpha-1}\pi^\alpha n^\alpha} \implies \mathcal{P}^{\text{Gauss}}[\{a_n, b_n\}] \\ &= \prod_{n=1}^{\infty} \frac{1}{2\pi\sigma_n^2} \exp\left[-\frac{1}{2} \frac{(a_n^2 + b_n^2)}{\sigma_n^2}\right] \quad (\text{full periodic series}). \end{aligned} \quad (6)$$

For the sine and the cosine series, the variances are

$$[\sigma_n^{\text{cos}}]^2 = [\sigma_n^{\text{sin}}]^2 = \frac{2L^{\alpha-1}}{\pi^\alpha n^\alpha}. \quad (7)$$

This choice leads to analogous expressions for the probability distributions $\mathcal{P}^{\text{Gauss}}[\{s_n\}]$ and $\mathcal{P}^{\text{Gauss}}[\{c_n\}]$, respectively.

The variances in equations (6) and (7) scale with the system size as $\propto L^{\alpha-1} = L^{2\zeta}$ where ζ is the roughness exponent. This exponent characterizes the main geometric properties of a self-affine system.

In this paper, we first consider Gaussian functions on the entire interval $[0, L]$. We compute the average of the width distribution for the three series and for general values of $\alpha > 1$ (section 2.1). The average of the width distribution strongly depends on the boundary conditions (for $\alpha \neq 2$). These results are then generalized (section 2.2) to the case when the function $u(t)$ is restricted to a window of width δ , in the interval $t/L \in [x, x + \delta]$:

$$w_2(x, \delta) = \frac{1}{L\delta} \int_{Lx}^{L(x+\delta)} dt u^2(t) - \left(\frac{1}{L\delta} \int_{Lx}^{L(x+\delta)} dt u(t) \right)^2. \quad (8)$$

These window boundary conditions are closer to the experimental situation than those realized by either the full periodic or the cosine series (see figure 2). We write (section 3) the characteristic function of the width distribution in terms of the eigenvalues of an infinite matrix which depends on the basis functions of the Fourier series, and on the window parameters $\{\delta, x\}$. In practice, to compute the width distribution for any of the series, in an arbitrary finite window, it suffices to compute this characteristic function from the eigenvalues of a finite-rank approximation of the above matrix, and to perform an inverse Fourier transform. It is easy to see that the width distribution depends on the size of the window and on the choice of boundary conditions. In the small-window limit ($\delta \rightarrow 0$ and far from the boundaries $\delta \ll \min[x, 1 - x]$), finite-rank approximations to the above matrix cease to be accurate (the limit of rank $N \rightarrow \infty$ does not commute with the limit $\delta \rightarrow 0$, for $\alpha < 3$), but we are able to write all the cumulants of the width distribution directly in this limit (section 3.3) via a subtle asymptotic expansion in powers of δ . We prove that in the small-window limit the width distribution becomes independent of the boundary condition. We also show how to practically compute the (α -dependent)

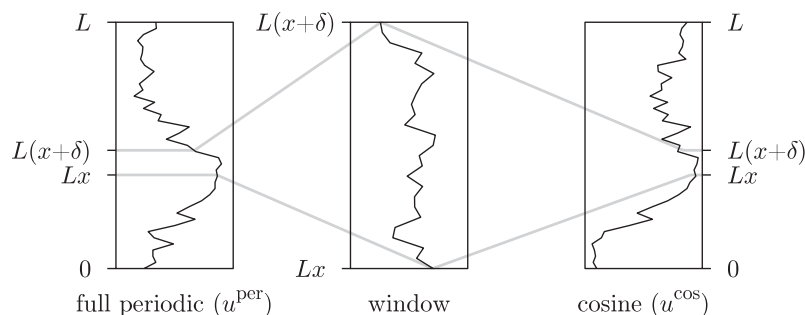


Figure 2. Gaussian functions $u^{\text{per}}(t)$ and $u^{\text{cos}}(t)$. Window boundary conditions correspond to picking out a piece of the function in the interval $t/L \in [x, x + \delta]$ and shifting it such that the window mean value vanishes. The width distribution in the small-window limit can belong to $u^{\text{per}}(t)$ or to $u^{\text{cos}}(t)$.

universal width distribution directly in this limit. For $\alpha > 3$ (section 3.3.2), the problem simplifies. The characteristic function in the small-window limit then corresponds to a matrix with only one non-zero eigenvalue and the corresponding width distribution no longer depends on α . We give its explicit form. Finally, we compute the logarithmic corrections to these asymptotic results for odd-integer values of α . In appendices A and B, we provide technical details of our calculation.

In a previous paper on the same subject [16], we already studied the second moment of the width distribution and presented arguments for the universality in the small-window limit. The more complete, and more concrete, calculations of the present paper rely on the representation of the characteristic function in terms of the spectrum of a matrix, which was not contained in [16].

2. Average width

In a self-affine (critical) system, the length L of the total interval is, as mentioned, the only characteristic length and the average value of the total width scales as $\langle w_2 \rangle \propto L^\zeta$ ($\langle \dots \rangle$ denotes the ensemble average).

2.1. Average width for $\delta = 1$

Fixing $\delta = 1$ and $x = 0$ in equation (8) and integrating over t yields

$$w_2 = \begin{cases} \frac{1}{2} \sum_{n=1}^{\infty} (a_n^2 + b_n^2) & \text{(full periodic series)} \\ \sum_{n=1}^{\infty} \left[\frac{1}{2} s_n^2 - \sum_{m=1}^{\infty} \frac{(1 - (-1)^m)(1 - (-1)^n) s_n s_m}{\pi^2 n m} \right] & \text{(sine series)} \\ \frac{1}{2} \sum_{n=1}^{\infty} c_n^2 & \text{(cosine series).} \end{cases}$$

From the Gaussian probability distributions given in equations (5)–(7), the ensemble averages are

$$\frac{\langle w_2 \rangle}{L^{\alpha-1}} = \begin{cases} \frac{2}{(2\pi)^\alpha} \zeta(\alpha) & \text{(full periodic series)} \\ \frac{1}{\pi^\alpha} \zeta(\alpha) - \frac{2}{\pi^2} \frac{2^{\alpha+2} - 1}{(2\pi)^\alpha} \zeta(\alpha + 2) & \text{(sine series)} \\ \frac{1}{\pi^\alpha} \zeta(\alpha) & \text{(cosine series),} \end{cases}$$

where $\zeta(x)$ is the Riemann Zeta function. For all α , the average width of the full periodic series is smaller than that of the cosine series, as is quite natural. For $\alpha = 2$, the average widths of the full periodic series and the sine series coincide, because the two differ only through boundary conditions for the derivative of u that a Markovian process is insensitive to.

2.2. Average width for $\delta < 1$

We now compute the average width for $\delta < 1$ for the full periodic series, the cosine and the sine series. The width $w_2^{\text{per}}(\delta)$ is independent of the origin x but the x dependence of the average width cannot be neglected in the other two cases. For the full periodic series, one obtains from equations (2) and (8)

$$w_2^{\text{per}}(\delta) = \sum_{n,m=1}^{\infty} a_n a_m C_{nm}(\delta) + a_n b_m I_{nm}(\delta) + b_n b_m S_{nm}(\delta), \quad (9)$$

where the coefficients $C_{nm}(\delta)$ are given by elementary integrals:

$$C_{mn} = \frac{1}{\delta} \int_x^{x+\delta} dt \cos(2\pi mt) \cos(2\pi nt) - \frac{1}{\delta^2} \int_x^{x+\delta} dt \cos(2\pi mt) \int_x^{x+\delta} dt \cos(2\pi nt). \quad (10)$$

Analogously, S_{nm} and I_{nm} can be expressed in terms of sine–sine and cosine–sine integrals. For the full periodic series, these coefficients are naturally independent of x .

Equation (9) allows us to compute w_2^{per} for one given sample. Integrating over the Gaussian Fourier components $\{a_n, b_n\}$, we get

$$\langle w_2^{\text{per}}(\delta) \rangle = \frac{L^{\alpha-1}}{2^{\alpha-1} \pi^\alpha} \sum_{n=1}^{\infty} \frac{C_{nn} + S_{nn}}{n^\alpha}, \quad \text{where } C_{nn} + S_{nn} = 1 - \frac{1 - \cos(2\pi n\delta)}{2(\pi n\delta)^2}. \quad (11)$$

The sum in equation (11) is easily evaluated for finite δ (see figure 3). The limit of this mean value for $\delta \rightarrow 0$ cannot be obtained by naive Taylor expansions of each term in this infinite sum in equation (11), because it is not uniformly convergent in the interval $\delta \in [0, 1]$ for $\alpha < 3$ (in the limit $\delta \rightarrow 0$, the terms of the sum behave as $(C_{nn}(\delta) + S_{nn}(\delta))n^{-\alpha} \sim \delta^2 n^{2-\alpha}$, producing a diverging series for $\alpha < 3$). As we will discuss in detail later, the higher cumulants of the width distribution are given by multiple infinite sums which present the same pathology as the sum in equation (11). To sum the series in the limit $\delta \rightarrow 0$, we have derived a very useful expansion formula which has the

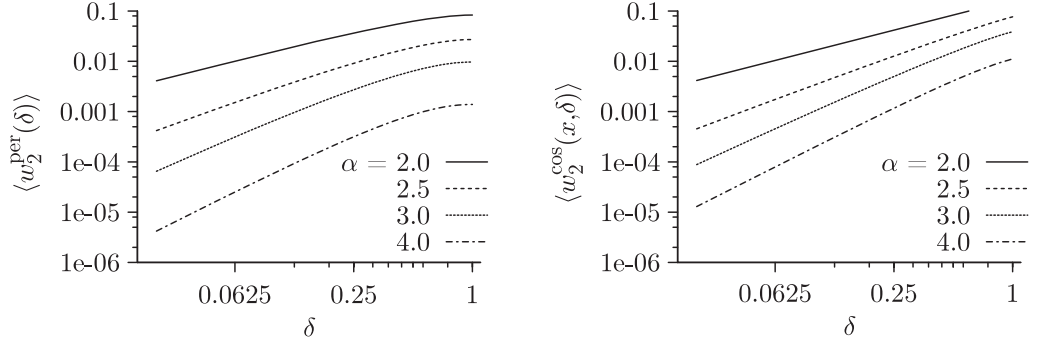


Figure 3. Mean square width as a function of window width, for different values of α , for the full periodic series (*left*) and the cosine series (*right*, with $x = \frac{1}{2}(1 - \delta)$) (from equations (11) and (16)).

same structure as the Euler–Maclaurin formula:

$$\sum_{n=1}^{\infty} \frac{f(n\delta)}{n^\alpha} = \delta^{\alpha-1} \int_0^\infty dt \left(\frac{f(t)}{t^\alpha} - \sum_{m=0}^{[\alpha]-1} \frac{f^{(m)}(0)t^{m-\alpha}}{m!} \right) + \sum_{m=0}^{\infty} \delta^m f^{(m)}(0) \frac{\zeta(\alpha - m)}{m!}, \quad (12)$$

where $[\alpha]$ is the integer part of α . Equation (12) holds inside the convergence radius $\delta = 1$ for all the quantities considered in this work (the formula is proved in appendix A). For analytic functions $f(z)$ and non-integer α , the first term on the right can be interpreted as the naive limit of the sum as $\delta \rightarrow 0$, with $t = n\delta$, whereas the second term contains the Taylor expansion of $f(n\delta)$ around zero. For integer α , the singularity of $\zeta(1)$ generates additional logarithms (see appendix A, again). Using the expansion formula of equation (12), one arrives at:

$$\frac{\langle w_2^{\text{per}}(\delta) \rangle}{L^{\alpha-1}} = \frac{2^{-\alpha-1}}{\zeta(-\alpha-1)} \frac{\zeta(\alpha+2)}{\pi^{\alpha+2}} \delta^{\alpha-1} + \frac{4}{(2\pi)^\alpha} \sum_{n=1}^{\infty} (-1)^{n+1} \frac{\zeta(\alpha-2n)}{(2n+2)!} (2\pi\delta)^{2n}. \quad (13)$$

To take into account the logarithmic corrections for odd integer α we must use equation (A.6) instead of equation (12). The final result is

$$\begin{aligned} \frac{\langle w_2^{\text{per}}(\delta) \rangle}{L^{\alpha-1}} &= (-1)^{(\alpha+1)/2} \frac{\psi_0(\alpha+2) - \log(2\pi\delta)}{2\pi(\alpha+1)!} \delta^{\alpha-1} \\ &+ \frac{4}{(2\pi)^\alpha} \sum_{n \neq (\alpha-1)/2} (-1)^{n+1} \frac{\zeta(\alpha-2n)}{(2n+2)!} (2\pi\delta)^{2n} \quad (\alpha \text{ odd integer}), \end{aligned}$$

where $\psi_0(z)$ is the digamma function. An expansion analogous to equation (13) appears in the correlation function governing the density of zero-crossings of a Gaussian function [10]. For integer-even α , the series in equation (13) is finite (because $\zeta(x) = 0$ for $x = \{-2, -4, \dots\}$). The mean square widths for the periodic random walk ($\alpha = 2$) and the driven curvature model ($\alpha = 4$) then have compact expressions:

$$\frac{\langle w_2^{\text{per}}(\delta) \rangle}{L^{\alpha-1}} = \begin{cases} \frac{1}{6}\delta - \frac{1}{12}\delta^2 & \text{for } \alpha = 2 \\ \frac{1}{144}\delta^2 - \frac{1}{120}\delta^3 + \frac{1}{360}\delta^4 & \text{for } \alpha = 4. \end{cases}$$

For the cosine series, we obtain, from equations (4) and (8), the mean squared width

$$w_2^{\cos}(x, \delta) = \sum_{n,m=1}^{\infty} c_n c_m D_{nm}(x, \delta), \quad (14)$$

where the coefficients are given by a symmetric matrix

$$D_{mn}(x, \delta) = \frac{1}{\delta} \int_x^{x+\delta} dt \cos(\pi mt) \cos(\pi nt) - \frac{1}{\delta^2} \int_x^{x+\delta} dt \cos(\pi mt) \int_x^{x+\delta} dt \cos(\pi nt). \quad (15)$$

D_{nm} is the overlap matrix of the basis functions in equation (4) on the interval $[x, x + \delta]$. For $\delta = 1$, the basis functions are, by construction, an orthonormal set and $D_{nm} = \frac{1}{2}\delta_{nm}$.

Integrating over the Gaussian variable $\{c_n\}$, the average width $\langle w_2^{\cos} \rangle$ becomes

$$\langle w_2^{\cos}(x, \delta) \rangle = \frac{2L^{\alpha-1}}{\pi^\alpha} \sum_{n=1}^{\infty} \frac{D_{nn}(x, \delta)}{n^\alpha}. \quad (16)$$

The sum in equation (16) is again easily evaluated for any value of x and δ . The behaviour of $\langle w_2^{\cos}(x, \delta) \rangle$ as a function of δ is shown in figure 3 for $x = \frac{1}{2}(1 - \delta)$. For small δ we notice that $\langle w_2^{\cos}(x, \delta) \rangle \propto \delta^{\alpha-1}$ for $\alpha < 3$ and $\langle w_2^{\cos}(x, \delta) \rangle \propto \delta^2$ for $\alpha > 3$. A special case is again $\alpha = 2$ where we have $\langle w_2^{\cos}(x, \delta) \rangle \propto \delta$ for all δ .

2.3. Small-window limit

In the following, we extract the universal behaviour of $\langle w_2^{\cos}(x, \delta) \rangle$ for a small window $[x, x + \delta]$ far from the boundaries (for $\delta \ll \min(x, 1 - x)$). For $\alpha < 3$, equation (16) can be expanded as

$$\langle w_2^{\cos}(x, \delta) \rangle = \frac{2L^{\alpha-1}}{\pi} \delta^{\alpha-1} \int_0^\infty dt \frac{D(t, x/\delta)}{t^\alpha} + O(\delta^2), \quad (17)$$

where the function $D(t, x/\delta)$ is obtained from the expression of $D_{nm}(x)$ by replacing $n\pi\delta \rightarrow t$. We write $D(t, x/\delta)$ as a sum of two terms:

$$D(t, x/\delta) = h(t, x/\delta) + \frac{1}{2} [C(t/2) + S(t/2)].$$

The function $h(t, x/\delta)$ contains all the x dependence of $D(t, x/\delta)$:

$$h\left(t, \frac{x}{\delta}\right) = \cos\left(2t\left(\frac{x}{\delta} + \frac{1}{2}\right)\right) \left[\frac{\sin(t)}{4t} - \frac{1}{t^2} \sin\left(\frac{t}{2}\right)^2 \right].$$

For $x/\delta \gg 1$, $h(t, x/\delta)$ oscillates rapidly and gives a vanishing contribution to the integral in equation (17). In particular, we can show that

$$\frac{\langle w_2^{\cos}(x, \delta) \rangle}{L^{\alpha-1}} \xrightarrow{x/\delta \rightarrow \infty} \frac{2^{-\alpha-1}}{\zeta(-\alpha-1)} \frac{\zeta(\alpha+2)}{\pi^{\alpha+2}} \delta^{\alpha-1} + O[\exp(-x/\delta)].$$

Comparing the above expression with equation (13), we conclude that, for $\alpha < 3$, the dominant contributions to $\langle w_2^{\cos}(x, \delta) \rangle$ and to $\langle w_2^{\text{per}}(\delta) \rangle$ coincide for small δ (compare also with figure 3). This conclusion can be extended to the sine series, where the explicit x dependence is again due to oscillatory terms that vanish in the small-window limit.

As mentioned before, the series in equation (16) is uniformly convergent for $\alpha > 3$, so that one can take the limit $\delta \rightarrow 0$ for each mode and then do the sum. Using the expansion

$$D_{nm}(x) = \frac{1}{12}nm\pi^2 \sin(\pi mx) \sin(\pi nx)\delta^2 + O(\delta^4) \quad (18)$$

in equation (16), we obtain

$$\frac{\langle w_2^{\cos}(x, \delta) \rangle}{L^{\alpha-1}} = \frac{1}{6} \left[\sum_{n=1}^{\infty} \frac{\sin^2(n\pi x)}{n^{\alpha-2}} \right] \pi^{2-\alpha} \delta^2 + O(\delta^{\alpha-1}, \delta^4). \quad (19)$$

For $x = 0$ and 1 , the δ^2 term vanishes, while for $0 < x < 1$ it is smaller than the corresponding term for the periodic case. This behaviour is consistent with the fact that, for $\alpha > 2$, the cosine series imposes vanishing derivatives at the end points. Hence these boundary conditions force $\langle w_2^{\cos} \rangle$ to be smaller than $\langle w_2^{\text{per}} \rangle$ for all $0 < x < 1$. The sine series gives a result analogous to the one for the cosine series. It suffices to replace the sine in the sum of equation (19) by a cosine.

3. Width distribution

The scaling behaviour of the average width gives access to the value of α and thus to the roughness exponent $\zeta = (\alpha - 1)/2$. However, the value of this exponent only depends on the two-point correlation functions and captures no finer geometric properties of the function $u(t)$. To discriminate between a Gaussian and a non-Gaussian function, one must have access to higher cumulants, as they are contained in the sample-to-sample fluctuations of the two-point correlation functions. The distribution $\mathcal{P}(w_2)$ has been used to analyse numerical and experimental data [13], [20]–[26]. The width distribution also allows us to estimate the roughness exponent from experimental data which are not sufficiently good to plot $\langle w_2(\delta) \rangle$ versus δ over several orders of magnitude in δ .

For general values of α , the width distribution has been computed for the entire interval ($\delta = 1, x = 0$), for the full periodic series, [17]–[19], and for the cosine series [13]. The underlying simplification with respect to the calculations in the present paper is that the matrix of coefficients for $\delta = 1$ satisfies $I_{nm} = 0$ while C_{nm} , S_{nm} , and D_{nm} are diagonal, as evident in equations (10) and (15). In order to study window boundary conditions (but also for the sine series), the previous framework must be generalized to non-diagonal matrices.

The width distribution can be obtained from the symmetric matrices

$$A_{nm}^{\cos} = 2\sigma_n^{\cos} D_{nm} \sigma_m^{\cos} \quad (20)$$

and

$$A^{\text{per}} = \begin{pmatrix} 2\sigma_n^{\text{per}} C_{nm} \sigma_m^{\text{per}} & \sigma_n^{\text{per}} I_{nm} \sigma_m^{\text{per}} \\ \sigma_n^{\text{per}} I_{mn} \sigma_m^{\text{per}} & 2\sigma_n^{\text{per}} S_{nm} \sigma_m^{\text{per}} \end{pmatrix}, \quad (21)$$

respectively. Concretely (see equations (9) and (14)), individual realizations of the mean square width distribution are generated by multiplying the matrices A in equations (20) and (21) by vectors of normal distributed Gaussian variables. This allows us to obtain $\mathcal{P}(w_2)$ approximately through direct simulation (see [15]).

On the other hand, one can compute all the moments of the distribution from contractions of a given matrix A (which can stand for A^{cos} , A^{sin} or A^{per}). For example, the second moment is given by

$$\mu_2 = \langle w_2^2 \rangle = \frac{1}{2} \sum_{n,m} A_{nm}^{\text{cos}} A_{mn}^{\text{cos}} + \frac{1}{4} \left(\sum_n A_{nn}^{\text{cos}} \right)^2 = \frac{1}{2} \text{Tr} [A^{\text{cos}}]^2 + \left[\frac{1}{2} \text{Tr} A^{\text{cos}} \right]^2. \quad (22)$$

Similar expressions exist for higher moments of the width distribution. As shown in appendix B, the cumulant κ_l of the rescaled width distribution, $\phi(z = w_2 / \langle w_2 \rangle) = \langle w_2 \rangle \mathcal{P}(w_2)$, can be expressed in a simpler way than the moments, as a trace of the matrix A taken to the l th power:

$$\kappa_l = \frac{(l-1)!}{2 \langle w_2 \rangle^l} \text{Tr} [A^l].$$

This is already apparent in equation (22), where $\mu_2 = \langle w_2 \rangle^2 (\kappa_2 + \kappa_1^2)$. The cumulants are thus given in terms of the normalized eigenvalues $\{\lambda_1, \lambda_2, \dots\}$ of the matrix A (the normalization condition corresponds to $\sum_k \lambda_k = 2$):

$$\kappa_l = \frac{(l-1)!}{2} \sum_k \lambda_k^l. \quad (23)$$

The cumulants in equation (23) yield an explicit formula for the cumulant-generating function $\Psi(s)$, where

$$\Psi(s) = \sum_{k=1}^{\infty} \sum_{l=1}^{\infty} \frac{\lambda_k^l}{2l} s^l = \sum_k \frac{1}{2} \log(1 - \lambda_k s).$$

The characteristic function $f(s) = \exp(\Psi(is))$, the exponential of the cumulant-generating function $\Psi(is)$, is given by

$$f(s) = \prod_k \frac{1}{\sqrt{1 - i\lambda_k s}}. \quad (24)$$

The spectrum of the matrices under consideration is such that the infinite product in equation (24) is uniformly convergent. The associated distribution is recovered through an inverse Fourier transform::

$$\phi(z) = \frac{1}{2\pi} \int_{-\infty}^{\infty} ds \exp(-izs) f(s), \quad (25)$$

which can be obtained by straightforward Riemann integration because the branch points $s_k = i/\lambda_k$ are away from the real axis.

3.1. Width distribution for the entire interval ($\delta = 1$)

As mentioned above, in the case $\delta = 1$, the matrices

$$A^{\text{per}} = \begin{pmatrix} [\sigma_n^{\text{per}}]^2 \delta_{nm} & 0 \\ 0 & [\sigma_n^{\text{per}}]^2 \delta_{nm} \end{pmatrix}, \quad \text{and} \quad A^{\text{cos}} = [\sigma_n^{\text{cos}}]^2 \delta_{nm}, \quad (26)$$

are diagonal and the computation of the cumulants from equation (23) is direct:

$$\kappa_l = \begin{cases} (l-1)! \zeta(l\alpha) / \zeta(\alpha)^l & \text{(full periodic series)} \\ (2l-2)!! \zeta(l\alpha) / \zeta(\alpha)^l & \text{(cosine series)}. \end{cases}$$

The cumulants for the sine series are more complicated because the corresponding matrix A^{sin} presents non-diagonal terms coming from the non-vanishing mean $(1/L) \int_0^L dt \sin(\pi n t / L)$ for odd values of n . The second cumulant, for example, is given by

$$\kappa_2^{\text{sin}} = \frac{2\zeta(2\alpha) + 2^{-2\alpha+1} (16\pi^{-4}(2^{\alpha+2} - 1)^2 \zeta(\alpha + 2)^2 - 8\pi^{-2}(2^{2\alpha+2} - 1)\zeta(2\alpha + 2))}{[\zeta(\alpha) - 2^{-\alpha+1}\pi^{-2}(2^{\alpha+2} - 1)\zeta(\alpha + 2)]^2}.$$

κ_2^{sin} agrees with κ_2^{per} only for $\alpha = 2$, as expected. In the case of the full periodic and the cosine series, the characteristic functions assume a simple form

$$f(s) = \begin{cases} \prod_k (1 - 2is / (\zeta(\alpha) k^\alpha))^{-1} & \text{(full periodic series)} \\ \prod_k (1 - 2is / (\zeta(\alpha) k^\alpha))^{-1/2} & \text{(cosine series)}. \end{cases}$$

As already discussed in [19], the twofold degeneracy of the spectrum of A^{per} for $\delta = 1$, evident in equation (26), yields a characteristic function $f(s)$ with simple poles on the imaginary axis. This simplifies the inverse Fourier transformation.

3.2. Width distribution for windows (finite δ)

The expressions allowing us to recover the width distribution from the eigenvalues of the matrices A^{cos} , A^{per} and A^{sin} remain valid for intervals $\delta < 1$, even though the computer must now be used for finite approximations of these infinite matrices, which are no longer diagonal. These calculations can be easily checked by direct simulation, as mentioned above. The outcome of this analysis is shown in figure 4 for the case $\alpha = 2.5$. It is evident that the width distribution changes with the sample size for the value of α chosen. Furthermore, the direct evaluation of the rescaled width distribution for finite but small δ suggests that this distribution becomes universal (independent of the boundary conditions) in the limit $\delta \rightarrow 0$. This scenario is confirmed by comparing the evolution of the (normalized) spectra of A^{per} and A^{cos} , as shown in figure 5.

We then compute $\phi(z)$ directly in the limit $\delta \rightarrow 0$. However, for small δ , increasingly larger matrices A^{per} and A^{cos} must be considered because of the non-uniform convergence of the traces of these matrices for $\delta \in [0, 1]$.

In section 3.3 we determine directly the width distribution in the limit $\delta \rightarrow 0$. In particular, analogously to the computation of asymptotics of the average width (section 2.3), the expansion formula equation (12) is proven useful to compute the cumulants of the distribution in the small-window limit for $\alpha < 3$ (section 3.3.1). This analysis serves two purposes: it proves the universality of the width distribution and provides a high-precision method to compute it directly in the limit $\delta \rightarrow 0$.

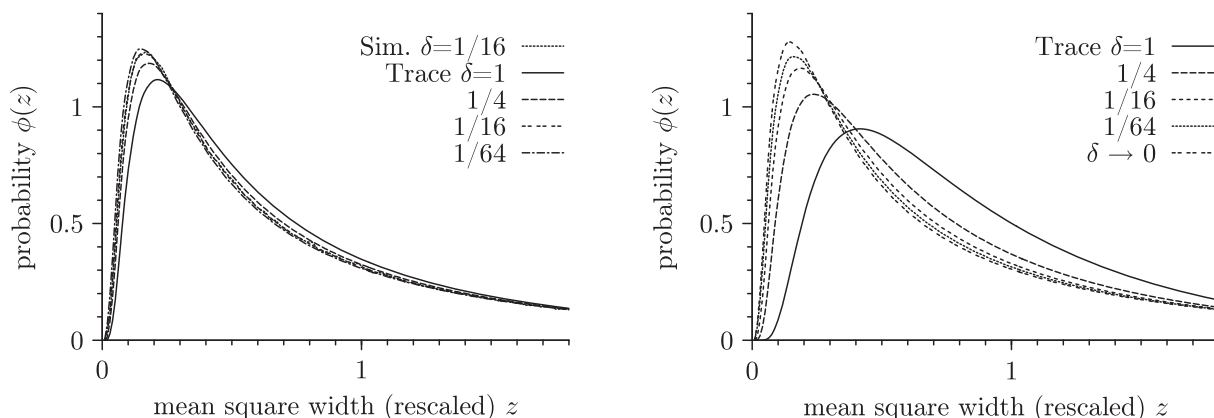


Figure 4. Rescaled probability distributions for the mean square width for $\zeta = 0.75$ ($\alpha = 2.5$) for the cosine series (*left*) and the full periodic series (*right*), obtained from equations (24) and (25). The result of direct simulations for $\delta = 1/16$ (from equation (14)) and the solution in the limit $\delta \rightarrow 0$ (from the matrix in equation (32)) are also shown. Sizes of the matrices are $N = 512$ and 1024 .

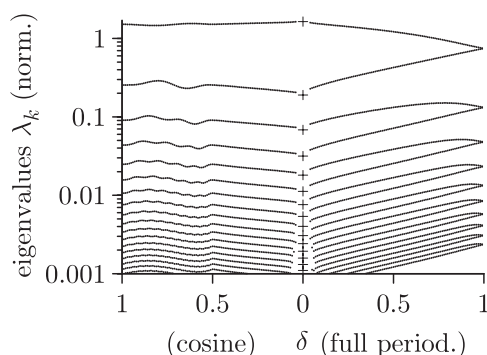


Figure 5. Eigenvalues $\{\lambda_1, \lambda_2, \dots\}$ for the cosine and the full periodic series as a function of window size δ ($\alpha = 2.5$ ($\zeta = 0.75$), for the cosine series, $x = \frac{1}{2}(1 - \delta)$). The spectrum in the small-window limit $\delta \rightarrow 0$ (*crosses*) is obtained in section 3.3. Eigenvalues are normalized as $\sum_k \lambda_k = 2$.

3.3. Width distribution in the small-window limit

In section 2.3 we computed the mean square widths $\langle w_2^{\text{per}}(\delta) \rangle$ and $\langle w_2^{\text{cos}}(x, \delta) \rangle$ in the small-window limit. We now determine the rescaled width distribution $\phi(z)$ in this limit.

3.3.1. Small-window limit ($\alpha < 3$). The computation of the cumulants κ_l of the rescaled width distribution as a δ -expansion is along the lines of the previous determination of $\langle w_2 \rangle$ (see equations (23)–(25) for the relation between the cumulants and the width distribution). For $\alpha < 3$, we handle the non-uniform convergence of the traces in equation (23) for $\delta \rightarrow 0$ using the expansion formula equation (12). The leading

contribution to κ_l , $l = 1, 2, \dots$, is given by multiple integrals:

$$\kappa_l^{\text{per}} = \frac{\pi^{l(\alpha-1)}(l-1)!}{2\widehat{w}_2^l} \int_0^\infty \cdots \int_0^\infty \prod_{n=1}^l \frac{dt_n}{t_n^\alpha} \text{Tr} [A^{\text{per}}(t_1, t_2) A^{\text{per}}(t_2, t_3) \cdots A^{\text{per}}(t_l, t_1)] + O(\delta^{3-\alpha}) \quad (27)$$

$$\begin{aligned} \kappa_l^{\text{cos}}(x/\delta) &= \frac{\pi^{l(\alpha-1)}(l-1)!}{2\widehat{w}_2^l} \int_0^\infty \cdots \int_0^\infty \prod_{n=1}^l \frac{dt_n}{t_n^\alpha} \\ &\quad \times \text{Tr} \left[A^{\text{cos}} \left(t_1, t_2, \frac{x}{\delta} \right) A^{\text{cos}} \left(t_2, t_3, \frac{x}{\delta} \right) \cdots A^{\text{cos}} \left(t_l, t_1, \frac{x}{\delta} \right) \right] + O(\delta^{3-\alpha}). \end{aligned} \quad (28)$$

In the above equations, \widehat{w}_2 is the prefactor of the leading term in the expansion of $\langle w_2(\delta, x) \rangle$, given in equation (13):

$$\widehat{w}_2 = \frac{(2)^{-\alpha-1} L^{\alpha-1} \zeta(\alpha+2)}{\zeta(-\alpha-1) \pi^{\alpha+2}},$$

which is independent of the boundary conditions. $A^{\text{cos}}(t_n, t_{n+1}, x/\delta)$ and $A^{\text{per}}(t_n, t_{n+1})$ are obtained by replacing $\pi n\delta$ with t_n in A^{cos} and in A^{per} . We now verify for each cumulant

$$\kappa_l^{\text{cos}} \xrightarrow{x/\delta \rightarrow \infty} \kappa_l^{\text{per}} + O(e^{-x/\delta}). \quad (29)$$

Extracting the x/δ -independent part of κ_l^{cos} one obtains

$$\begin{aligned} \kappa_l^{\text{cos}} &= \frac{\pi^{l(\alpha-1)}(l-1)!}{2\widehat{w}_2^l} \int_0^\infty \cdots \int_0^\infty \prod_{n=1}^l \frac{dt_n}{t_n^\alpha} \text{Tr} \left[\tilde{A}^{\text{cos}}(t_1, t_2) \tilde{A}^{\text{cos}}(t_2, t_3) \cdots \tilde{A}^{\text{cos}}(t_l, t_1) \right] \\ &\quad + \text{oscill. terms}, \end{aligned} \quad (30)$$

where \tilde{A}^{cos} is now independent of x and given by

$$\tilde{A}^{\text{cos}}(t, t') = \frac{4L^{\alpha-1}}{\pi^\alpha} \begin{pmatrix} \frac{1}{2(t-t')} \sin \frac{t-t'}{2} - \frac{1}{tt'} \sin \frac{t}{2} \sin \frac{t'}{2} & \frac{1}{2(t+t')} \sin \frac{t+t'}{2} - \frac{1}{tt'} \sin \frac{t}{2} \sin \frac{t'}{2} \\ \frac{1}{2(t+t')} \sin \frac{t+t'}{2} - \frac{1}{tt'} \sin \frac{t}{2} \sin \frac{t'}{2} & \frac{1}{2(t-t')} \sin \frac{t-t'}{2} - \frac{1}{tt'} \sin \frac{t}{2} \sin \frac{t'}{2} \end{pmatrix}. \quad (31)$$

Now it is straightforward to verify that the matrices A^{per} and A^{cos} satisfy

$$\begin{aligned} &\text{Tr} \left[\tilde{A}^{\text{cos}}(t_1, t_2) \tilde{A}^{\text{cos}}(t_2, t_3) \cdots \tilde{A}^{\text{cos}}(t_l, t_1) \right] \\ &= 2^{l(\alpha-1)} \text{Tr} [A^{\text{per}}(t_1/2, t_2/2) A^{\text{per}}(t_2/2, t_3/2) \cdots A^{\text{per}}(t_l/2, t_1/2)]. \end{aligned}$$

This establishes the validity of equation (29).

Closed analytic expressions have not been obtained for the above integrals. Actually the problem of computing the integrals in equation (30) reduces to the solution of a homogeneous Fredholm equation of the second kind:

$$\int_0^\infty dt \sum_{j=1}^2 \tilde{A}^{\text{cos}}(t, t')_{ij} g_j(t') = \lambda g_i(t),$$

where the 2×2 matrix $\tilde{A}^{\text{cos}}(t, t')$ is a compact kernel with a discrete set of eigenvalues λ_k converging to 0, which encode all the information on the cumulants κ_l , in the same way as for the discrete case (equation (23)).

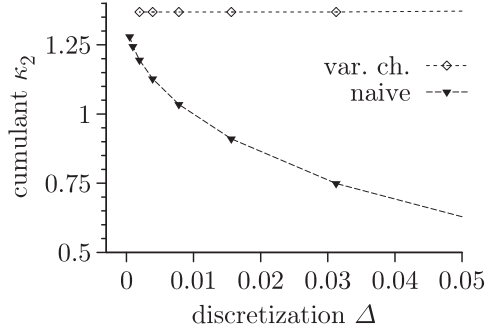


Figure 6. Cumulant κ_2 of the rescaled width distribution for $\alpha = 2.5$ from a naive discretization of the integral in equation (30), and after the change of variables in equation (32) (Riemann integration in the interval $t \in [0, 15]$, using $\Delta = t_{i+1} - t_i$).

The spectrum of the kernel $\tilde{A}^{\cos}(t, t')$ is most easily obtained by discretizing the variables t and t' on an equally spaced grid with $t_k = \Delta(k - \frac{1}{2})$, $k = 1, \dots, N$, with an upper cut-off for the integrations. However, the singularities of the integrands makes the convergence rather slow ($\sim t_n^{2-\alpha}$ for $t_n \rightarrow 0$ (with all other variables kept finite)). The divergence in the integrals at small t is eliminated by a standard change of variables: an integral of a function diverging as $1/t^\gamma$ for $t \rightarrow 0$ can be written as

$$\int_0^\infty dt f(t) = \frac{1}{1-\gamma} \int_0^\infty dt t^{\gamma/(1-\gamma)} f[t^{1/(1-\gamma)}].$$

The integrand on the right is constant for small t . Concretely, the change of variables in \tilde{A}^{\cos} leads to a matrix

$$\tilde{A}^{\cos}(t, t') = \frac{1}{3-\alpha} t^{(\alpha-2)/(6-2\alpha)} \tilde{A}^{\cos}(t^{1/(3-\alpha)}, t'^{1/(3-\alpha)}) t'^{(\alpha-2)/(6-2\alpha)}, \quad (32)$$

which can again be discretized. The characteristic function of the width distribution is computed from the spectrum of the $2N \times 2N$ matrix \tilde{A}^{\cos} as discussed before. To show what is gained by rescaling the matrix \tilde{A} in equation (31), we have computed the second cumulant κ_2 on an equally spaced grid with both versions (see figure 6). The rescaled matrices converge exceptionally well with the discretization parameter Δ . In figure 5, the spectrum of the rescaled kernel (for $\delta \rightarrow 0$) is compared to the spectra of A^{per} and A^{\cos} for finite δ . Only in the special case $\alpha = 2$ is the spectrum of the cosine series independent of δ , because of the Markov-chain property of the random walk. For all $\alpha \neq 2$, the spectrum depends on δ , but the cumulants of the width distribution satisfy

$$\kappa_l^{\text{per}}(\delta \rightarrow 0) = \kappa_l^{\cos}(\delta \rightarrow 0) \neq \kappa_l^{\cos}(\delta = 1),$$

in a way illustrated in figure 5. As was already shown in figure 4 for $\alpha = 2.5$, the convergence of the width distribution for finite δ towards the asymptotic width distribution is quite fast, even though the rate of convergence depends on the value of α .

3.3.2. Small-window limit ($\alpha \geq 3$). For $\alpha \geq 3$, the integral term in equation (12) is subdominant, and the naive expansion of the matrices A^{per} and A^{\cos} in powers of δ becomes

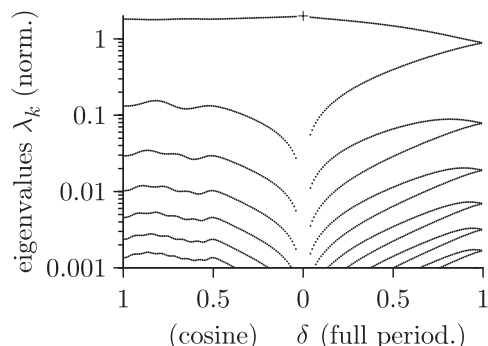


Figure 7. Eigenvalue spectrum of A^{cos} and A^{per} for $\alpha = 3.5$ ($\zeta = 1.25$). A single eigenvalue remains non-zero in the limit $\delta \rightarrow 0$ (*cross*). The normalization condition $\lambda_1 = \sum_k \lambda_k = 2$ corresponds to the rescaling of the width distribution, with $\langle w_2 \rangle = 1$.

correct in the limit $\delta \rightarrow 0$. Using the expansions in equation (18) and, furthermore,

$$C_{mn} = O(\delta^4), \quad S_{mn} = \frac{1}{3}mn\pi^2\delta^2 + O(\delta^4), \quad I_{nm} = O(\delta^3), \quad (33)$$

we can construct the matrices A^{per} and A^{cos} , and check that they have only a single non-zero eigenvalue. For illustration, we show in figure 7 the spectrum of these two matrices for $\alpha = 7/2$ at finite δ (eigenvalues are normalized so that $\sum_k \lambda_k = 2$).

From equation (23) we then obtain

$$\kappa_l^{\text{cos}}(\delta \rightarrow 0) = \kappa_l^{\text{per}}(\delta \rightarrow 0) = \begin{cases} (2l - 2)!! + O(\delta^{\alpha-3}) & \text{for } \alpha > 3 \\ (2l - 2)!! + O(1/\log \delta) & \text{for } \alpha = 3. \end{cases}$$

The associated characteristic function is

$$f(s) = (1 - 2is)^{-1/2},$$

and its inverse Fourier transform gives the universal distribution $\mathcal{P}(z)$ for $\alpha > 3$:

$$\phi(z) = \frac{\exp[-z/2]}{\sqrt{2\pi z}}.$$

By comparing the universal distribution for $\alpha > 3$ with the ones with $\alpha < 3$ (see figure 4), one notices that the additional eigenvalues (and branch points contributing to the characteristic function) allow the distribution $\phi(z)$ to vanish at $z = 0$, thus producing a local maximum in this function.

4. Conclusions

In conclusion, we have studied the geometric properties of functions with a particularly simple expression in Fourier space: independent Gaussian random variables. We have restricted ourselves to one-dimensional self-affine functions (characterized by a single length scale), but our analysis evidently carries over to functions with more than one length scale, and to higher dimensions. In real space, the geometrical properties are non-trivial, and the boundary conditions play an important role. This comes about because

the real-space action, for all non-even α , contains non-local operators and, for all $\alpha \neq 2$, is non-Markovian.

We have provided a simple and compact framework for studying the boundary effects for general non-Markovian Gaussian processes by relating the characteristic function of the width distribution to the spectrum of boundary-dependent infinite matrices, which essentially encode the overlap of the basis functions of the Fourier series. The choice of Fourier basis (resulting in the full periodic, cosine and sine series) determines the different boundary conditions. We have carried out a complete analysis of the spectrum of these matrices for different values of α for the case of the function on the entire interval and also for the function restricted to a window. The associated width distributions could all be determined by solving for the eigenvalues of a matrix, and by performing a straightforward inverse Fourier transform.

We have shown that the non-Markovian action propagates the effects of boundary conditions over the entire interval. However, in the small-window limit, the width distribution becomes universal (independent of boundary conditions). For $\alpha < 3$, we showed how to compute the cumulants of the width distribution in this limit, avoiding problems related to the non-uniform convergence of the Fourier series. For $\alpha > 3$, the problem of finding the universal width distribution drastically simplifies and we were able to write it down explicitly. Finally, we have obtained the logarithmic corrections in the case of odd-integer α , in particular for $\alpha = 3$.

We hope that our work will be useful for the analysis of experimental data (which usually correspond to our window boundary conditions, often in the regime $\delta \rightarrow 0$, which we found to be universal). In many experiments, the roughness exponent cannot be extracted reliably by extrapolation, and the width distribution may provide crucial additional information.

Computer programs that compute the width distributions for any value of α , both at finite δ and in the limit $\delta \rightarrow 0$, are available [27]. These programs allow us to construct the width distributions for all values of ζ and δ . Experimental data should be fitted with these functions (preferentially in the $\delta \rightarrow 0$ limit). Note that this procedure has already been applied [13], even though, at the time, the role of boundary conditions was not clearly understood.

Acknowledgments

The authors thank the Kavli Institute for Theoretical Physics, Santa Barbara, for its hospitality. This research was supported in part by the National Science Foundation under Grant No. PHY99-07949.

Appendix A. Expansion formula

In this appendix we derive the expansion formula of equation (12), first for non-integer, then for integer values of α .

A.1. Expansion formula for non-integer α

We consider the sum

$$\sum_{n=1}^{\infty} \frac{f(n\delta)}{n^{\alpha}},$$

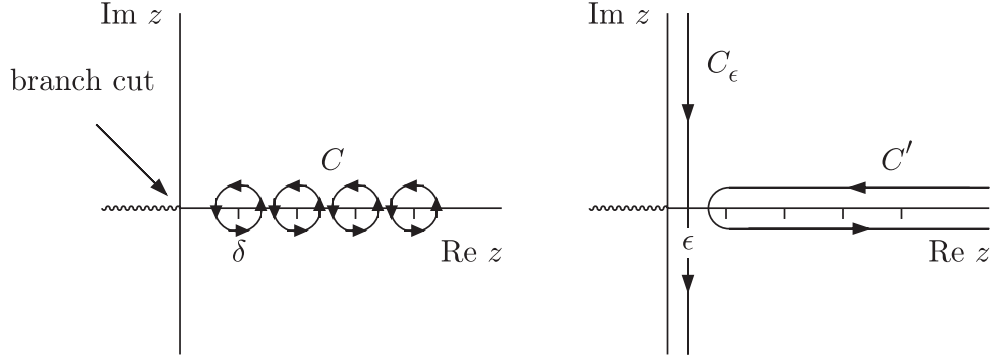


Figure A.1. Contours for the integral in equation (A.2). The indicated deformation of the contour ($C \rightarrow C' \rightarrow C_\epsilon$) transforms equation (A.2) into equation (A.3).

where $f(z)$ is assumed to be a general analytic function. In order to obtain the expansion in powers of δ of the above sum, we expand $f(z)$:

$$\sum_{n=1}^{\infty} \frac{f(n\delta)}{n^\alpha} = \sum_{n=1}^{\infty} \sum_{m=0}^{\infty} \frac{f^{(m)}(0)}{m! n^{\alpha-m}} \delta^m.$$

For $\alpha - m < 1$, the sum over n converges and can be directly evaluated using the Riemann Zeta function $\zeta(\alpha - m) = \sum_n 1/n^{\alpha-m}$:

$$\sum_{n=1}^{\infty} \frac{f(n\delta)}{n^\alpha} = \sum_{m=0}^{[\alpha]-1} \frac{f^{(m)}(0)\zeta(m-\alpha)}{m!} \delta^m + \sum_{n=1}^{\infty} \frac{\tilde{f}(n\delta)}{n^\alpha}, \quad (\text{A.1})$$

where $[\alpha]$ is the integer part of α and $\tilde{f}(z) = \sum_{[\alpha]}^{\infty} f^{(m)}(0)z^m/m!$. The second term on the right-hand side of equation (A.1) can be expressed as a contour integral in the complex plane:

$$\sum_{n=1}^{\infty} \frac{\tilde{f}(n\delta)}{n^\alpha} = \frac{\delta^{\alpha-1}}{2i} \int_C dz \frac{\tilde{f}(z)}{z^\alpha} \cot\left(\frac{\pi}{\delta}z\right), \quad (\text{A.2})$$

where the contour C encircles the poles $z_n = n\delta$, $n = 1, 2, \dots$ of the function $G(z) = [\tilde{f}(z)/z^\alpha] \cot(\pi z/\delta)$. The contour C is transformed into the contour C_ϵ , as shown in figure A.1, avoiding the branch point at the origin. By considering the integration over the contour C_ϵ , and by performing the change of variables $z \rightarrow -i(z/\delta - \epsilon)$, we have:

$$\sum_{n=1}^{\infty} \frac{\tilde{f}(n\delta)}{n^\alpha} = -\frac{i}{2} \int_{-\infty}^{\infty} dz \frac{\tilde{f}[\delta(i z + \epsilon)]}{(i z + \epsilon)^\alpha} \coth[\pi(z - i\epsilon)]. \quad (\text{A.3})$$

To extract the δ -series of the above integral, it is tempting to integrate term by term the Taylor series of the function $\tilde{f}(z)$. We first split the above integral into the following

terms:

$$\begin{aligned} \sum_{n=1}^{\infty} \frac{\tilde{f}(n\delta)}{n^\alpha} &= -\frac{i}{2} \int_0^\infty dz \tilde{f}[\delta(iz + \epsilon)](iz + \epsilon)^{-\alpha} [\coth[\pi(z - i\epsilon)] - 1] \\ &\quad - \frac{i}{2} \int_0^\infty dz \tilde{f}[\delta(iz + \epsilon)](iz + \epsilon)^{-\alpha} \\ &\quad - \frac{i}{2} \int_{-\infty}^0 dz \tilde{f}[\delta(iz + \epsilon)](iz + \epsilon)^{-\alpha} [\coth[\pi(z - i\epsilon)] + 1] \\ &\quad + \frac{i}{2} \int_{-\infty}^0 dz \tilde{f}[\delta(iz + \epsilon)](iz + \epsilon)^{-\alpha}. \end{aligned}$$

This separation is valid if all the above integrals are well defined, a condition respected by the functions $f(z)$ considered in this paper (for $\delta \leq 1$). Using the following representation of the Riemann Zeta function, valid for $\text{Re}(\beta) < 1$:

$$\zeta(\beta) = \lim_{\epsilon \rightarrow 0} \left(-\frac{i}{2} \left[\int_0^\infty dz (iz + \epsilon)^{-\beta} (\coth[\pi(z - i\epsilon)] - 1) + \int_{-\infty}^0 dz (iz + \epsilon)^{-\beta} (\coth[\pi(z - i\epsilon)] + 1) \right] \right),$$

we obtain

$$\begin{aligned} \sum_{n=1}^{\infty} \frac{\tilde{f}(n\delta)}{n^\alpha} &= \sum_{m=[\alpha]}^{\infty} \frac{f^{(m)}(0)}{m!} \delta^m \zeta(\alpha - m) + \frac{-i}{2} \int_0^\infty dz \tilde{f}(z)(iz + \epsilon)^{-\alpha} \\ &\quad + \frac{i}{2} \int_{-\infty}^0 dz \tilde{f}(z)(iz + \epsilon)^{-\alpha}. \end{aligned} \quad (\text{A.4})$$

Finally, by considering the contours shown in figure A.2, we verify that

$$\lim_{\epsilon \rightarrow 0} -\frac{i}{2} \int_0^\infty dz \tilde{f}(\delta(iz + \epsilon))(iz + \epsilon)^{-\alpha} + \frac{i}{2} \int_{-\infty}^0 dz \tilde{f}(\delta(iz + \epsilon))(iz + \epsilon)^{-\alpha} = \delta^{\alpha-1} \int_0^\infty dt \frac{\tilde{f}(t)}{t^\alpha}.$$

Collecting these results proves equation (12).

A.2. Expansion formula for integer α

The series in equation (12) is not defined for integer $\alpha = m + 1$, because of the simple pole of the Riemann Zeta function $\zeta(z)$ at $z = 1$. However, this divergence is compensated by an ultraviolet divergence in the integral. We analyse this situation by considering $\alpha = [\alpha] + \rho$, and by taking the limit $\rho \rightarrow 0$. We write:

$$\delta^{[\alpha]-1+\rho} \int_0^\infty dt \left(\frac{f(t)}{t^\alpha} - \sum_{m=0}^{[\alpha]-1} \frac{f^{(m)}(0)t^{m-[\alpha]+\rho}}{m!} \right) + \delta^{[\alpha]-1} \frac{f^{(\alpha-1)}(0)}{(\alpha-1)!} \zeta(1+\rho). \quad (\text{A.5})$$

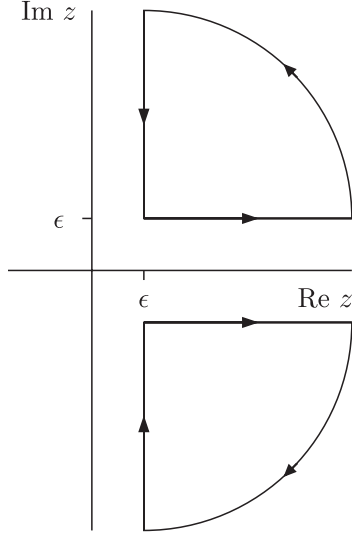


Figure A.2. Contours of the integrals in equation (A.4).

In order to isolate the ultraviolet divergence, we split the integral into two infrared-divergent terms, and equation (A.5) becomes

$$\delta^{[\alpha]+\rho-1} \int_{\epsilon}^{\infty} dt \left(\frac{f(t)}{t^{\alpha}} - \sum_{m=0}^{[\alpha]-2} \frac{f^{(m)}(0)t^{m-\alpha}}{m!} \right) - \delta^{[\alpha]+\rho-1} \int_{\epsilon}^{\infty} dt \frac{f^{(\alpha-1)}(0)}{(\alpha-1)!t^{1+\rho}} + \delta^{[\alpha]-1} \frac{f^{(\alpha-1)}(0)}{(\alpha-1)!} \zeta(1+\rho),$$

where ϵ is an infrared cut-off. Using the expansion $\zeta(1+\rho) = 1/\rho + \gamma + O(\rho)$, where γ is the Euler constant, we can take the limit $\rho \rightarrow 0$:

$$\lim_{\rho \rightarrow 0} \left[\zeta(1+\rho) - \delta^{\rho} \int_{\epsilon}^{\infty} dt \frac{1}{t^{1+\rho}} \right] = [\gamma - \log(\delta) - \log(\epsilon)].$$

From the above we get the following expansion formula for integer values of α :

$$\sum_{n=1}^{\infty} \frac{f(n\delta)}{n^{\alpha}} = \delta^{\alpha-1} \left(\text{const} - \frac{f^{(\alpha-1)}(0)}{(\alpha-1)!} \log(\delta) \right) + \sum_{m \neq \alpha-1} \delta^m f^{(m)}(0) \frac{\zeta(\alpha-m)}{m!}, \quad (\text{A.6})$$

where the constant is expressed in terms of the following limit:

$$\text{const} = \lim_{\epsilon \rightarrow 0} \left(\int_{\epsilon}^{\infty} dt \left(\frac{f(t)}{t^{\alpha}} - \sum_{m=0}^{\alpha-2} \frac{f^{(m)}(0)t^{m-\alpha}}{m!} \right) + \frac{f^{(\alpha-1)}(0)}{(\alpha-1)!} (\log(\epsilon) + \gamma) \right).$$

Appendix B. General cumulants

For completeness, we derive in this appendix the trace formula for the cumulants κ_l of the rescaled width distribution $\Psi(s)$ for all l from their generating function

$$\Psi(s) = \log \langle \exp(sz) \rangle = \sum_{l=1}^{\infty} \frac{\kappa_l}{l!} s^l.$$

We first consider the full periodic series. To compute the average $\langle \exp(sz) \rangle$ we have to integrate over the Gaussians $\{a_n, b_n\}$. To make all the Gaussian integrals well defined, we introduce a cut-off N in the momentum space, such that $n = 1, \dots, N$. The average $\langle \exp(sz) \rangle$ takes the form:

$$\langle \exp(sz) \rangle = \frac{\left(\prod_{n'} \int_{-\infty}^{\infty} dx_{n'} \right) \exp[-\frac{1}{2} \sum_{n'm'} M_{n'm'}(s) x_{n'} x_{m'}]}{\left(\prod_{n'} \int_{-\infty}^{\infty} dx_{n'} \right) \exp[-\frac{1}{2} \sum_{n'm'} M_{n'm'}(0) x_{n'} x_{m'}]} = \left[\frac{\text{Det } M(s)}{\text{Det } M(0)} \right]^{-1/2},$$

where the indices n' and m' run from 0 to $2N$. In the above expression, we set $x_{n'} = a'_n$, for $n' = 0, \dots, N$ and $x_{n'} = b_{n'-N}$ for $n' = N + 1, \dots, 2N$. The matrix $M(s)$ is a block of four $N \times N$ matrices defined as

$$M(s) = \begin{pmatrix} \sigma_n^{-2} \delta_{nm} & 0 \\ 0 & \sigma_n^{-2} \delta_{nm} \end{pmatrix} - \frac{s}{\langle w_2^{\text{per}} \rangle} \begin{pmatrix} 2C_{nm} & I_{nm} \\ I_{mn} & 2S_{nm} \end{pmatrix}$$

(for the coefficients C_{nm} , I_{nm} and S_{nm} , see equation (9)). We arrive at the following expression for the $\Psi(s)$:

$$\Psi(s) = -\frac{1}{2} \log \text{Det } M(s) + \frac{1}{2} \log \text{Det } M(0) = -\frac{1}{2} \text{Tr}[\log M(s)] + \frac{1}{2} \text{Tr}[\log M(0)].$$

Expanding the logarithm $\log M(s)$ one obtains

$$\Psi(s) = \sum_{l=1}^{\infty} \frac{\text{Tr}[(A^{\text{per}})^l]}{2l \langle w_2^{\text{per}} \rangle^l} s^l,$$

where A^{per} is given in equation (21). Hence the l th cumulant of the roughness is given by

$$\kappa_l^{\text{per}} = \frac{(l-1)!}{2 \langle w_2^{\text{per}} \rangle^l} \text{Tr}[(A^{\text{per}})^l]. \quad (\text{B.1})$$

For the cosine series, one has to integrate over the Gaussian variables $\{c_n\}$ and $\{s_n\}$. One arrives at an analogous expression for the cumulants.

References

- [1] Toroczkai Z and Williams E D, 1999 *Phys. Today* **52** 24
- [2] Kardar M, 1998 *Phys. Rep.* **301** 85
- [3] Frisch U, 1995 *Turbulence: The Legacy of A. N. Kolmogorov* (Cambridge: Cambridge University Press)
- [4] Surya C (ed) 1999 *Proc. 15th Int. Conf. on Noise in Physical Systems and 1/f Fluctuations (IEEE Proceedings)*
- [5] Rosso A, Krauth W, Le Doussal P, Vannimenus J and Wiese K J, 2003 *Phys. Rev. E* **68** 036128
- [6] Le Doussal P and Wiese K J, 2003 *Phys. Rev. E* **68** 046118
- [7] Oldham K B and Spanier J, 1974 *The Fractional Calculus: Integrations and Differentiations of Arbitrary Order* (New York: Academic)
- [8] Majumdar S N, 2005 *Curr. Sci.* **89** 2076
- [9] Khare S V and Einstein T L, 1998 *Phys. Rev. B* **57** 4782
- [10] Majumdar S N and Bray A J, 2001 *Phys. Rev. Lett.* **86** 3700
- [11] Majumdar S N and Comtet A, 2004 *Phys. Rev. Lett.* **92** 225501
- [12] de Queiroz S L A, 2005 *Phys. Rev. E* **71** 016134
- [13] Moulinet S, Rosso A, Krauth W and Rolley E, 2004 *Phys. Rev. E* **69** 035103(R)
- [14] Feynman R P, 1972 *Statistical Mechanics* (New York: Addison-Wesley)
- [15] Krauth W, 2006 *Statistical Mechanics: Algorithms and Computations* (Oxford: Oxford University Press) (see www.phys.ens.fr/doc/SMAC)
- [16] Rosso A, Santachiara R and Krauth W, 2005 *J. Stat. Mech.* **L08001**

- [17] Foltin G, Oerding K, Rácz Z, Workman R L and Zia R K P, 1994 *Phys. Rev. E* **50** R639
- [18] Plischke M, Rácz Z and Zia R K P, 1994 *Phys. Rev. E* **50** 3589
- [19] Antal T, Droz M, Györgyi G and Rácz Z, 2001 *Phys. Rev. E* **65** 046140
- [20] Bramwell S T *et al*, 2000 *Phys. Rev. Lett.* **84** 3744
- [21] Bramwell S T *et al*, 2001 *Phys. Rev. E* **63** 041106
- [22] Marinari E, Pagnani A, Parisi G and Rácz Z, 2002 *Phys. Rev. E* **65** 026136
- [23] Vandembroucq D and Roux S, 2004 *Phys. Rev. E* **70** 026103
- [24] Zapperi S, Nukala P K V V and Šimunović S, 2005 *Phys. Rev. E* **71** 026106
- [25] Leschhorn H and Tang L, 1993 *Phys. Rev. Lett.* **70** 2973
- [26] Jensen H J, 1995 *J. Phys. A: Math. Gen.* **28** 1861
- [27] See www.lps.ens.fr/~krauth